



No observed developmental effects in early life stages of capelin (*Mallotus villosus*) exposed to a water-soluble fraction of crude oil during embryonic development

Jasmine Nahrgang, Cassandra Granlund, Morgan Lizabeth Bender, Lisbet Sørensen, Michael Greenacre & Marianne Frantzen

To cite this article: Jasmine Nahrgang, Cassandra Granlund, Morgan Lizabeth Bender, Lisbet Sørensen, Michael Greenacre & Marianne Frantzen (2023) No observed developmental effects in early life stages of capelin (*Mallotus villosus*) exposed to a water-soluble fraction of crude oil during embryonic development, *Journal of Toxicology and Environmental Health, Part A*, 86:12, 404-419, DOI: [10.1080/15287394.2023.2209115](https://doi.org/10.1080/15287394.2023.2209115)

To link to this article: <https://doi.org/10.1080/15287394.2023.2209115>



© 2023 The Author(s). Published with license by Taylor & Francis Group, LLC.



[View supplementary material](#)



Published online: 12 May 2023.



[Submit your article to this journal](#)



Article views: 593



[View related articles](#)



[View Crossmark data](#)

No observed developmental effects in early life stages of capelin (*Mallotus villosus*) exposed to a water-soluble fraction of crude oil during embryonic development

Jasmine Nahrgang ^a, Cassandra Granlund ^a, Morgan Lizabeth Bender ^{a,b,c}, Lisbet Sørensen ^d, Michael Greenacre ^e, and Marianne Frantzen ^b

^aDepartment of Arctic and Marine Biology, UiT The Arctic University of Norway, Tromsø, Norway; ^bAkvaplan-niva, Fram Centre, Tromsø, Norway; ^cOwl Ridge Natural Resource Consultants, Inc, Anchorage, USA; ^dClimate and Environment, SINTEF Ocean, Trondheim, Norway; ^eDepartment of Economics and Business, Universitat Pompeu Fabra, and Barcelona School of Management, Barcelona, Spain

ABSTRACT

The rise in offshore oil and gas operations, maritime shipping, and tourism in northern latitudes enhances the risk of oil spills to sub-Arctic and Arctic coastal environments. Therefore, there is a need to understand the potential adverse effects of petroleum on key species in these areas. Here, we investigated the effects of oil exposure on the early life stages of capelin (*Mallotus villosus*), an ecologically and commercially important Barents Sea forage fish species that spawns along the coast of Northern Norway. Capelin embryos were exposed to five different concentrations (corresponding to 0.5–19 µg/L total PAHs) of water-soluble fraction (WSF) of crude oil from 6 days post fertilization (dpf) until hatch (25 dpf), and development of larvae in clean seawater was monitored until 52 dpf. None of the investigated endpoints (embryo development, larval length, heart rate, arrhythmia, and larval mortality) showed any effects. Our results suggest that the early life stages of capelin may be more robust to crude oil exposure than similar life stages of other fish species.

KEYWORDS



Capelin; crude oil; early life stage; embryo; larvae


Introduction

As Arctic and sub-Arctic waters become increasingly accessible as a result of a warming climate, offshore oil and gas operations, maritime shipping, and other human activities are all expected to increase over the coming years (Eliasson et al. 2017). Ship traffic in the Arctic region has increased since 2012, especially in the Barents Sea and along the Northern Sea Route (Eguíluz et al. 2016; Hreinsson 2020; Smith and Stephenson 2013), which traverses feeding, wintering, and spawning areas for Arctic key species such as the capelin (*Mallotus villosus*) (Hop and Gjørseter 2013). Capelin, a pelagic fish with a circumpolar distribution throughout regions of the Pacific and Atlantic Oceans, has long been recognized as an essential forage and commercial fish species in the Northwest Atlantic ecosystem and constitutes the largest stock of pelagic fish in the Barents Sea (Hop and Gjørseter 2013). Capelin spawns 1 mm

demersal eggs that adhere to the spawning substrate in subtidal waters or on beaches along the North Norwegian and Northwestern Russian coasts (Hop and Gjørseter 2013). During the 1.5–2.5-month period from spawning until the hatched larvae swim out to the open sea beach-spawning capelin may be particularly vulnerable to exposure to spilled crude oil and its water-soluble fraction (WSF).

Crude oil can affect developing fish through multiple pathways, including cardiotoxicity (e.g., bradycardia, arrhythmia, and cardiac malformation), leading to developmental deformities and sublethal effects that may persist to later life stages (Hicken et al. 2011; Incardona et al. 2015, 2021; Mager et al. 2014). Recent studies have also highlighted the impairment of the neurological pathway in fish early life stages exposed to crude oil, independent of the cardiotoxic pathway (Greer et al.

CONTACT Jasmine Nahrgang  jasmine.m.nahrgang@uit.no  Department of Arctic and Marine Biology, UiT The Arctic University of Norway, Tromsø 9037, Norway

 Supplemental data for this article can be accessed online at <https://doi.org/10.1080/15287394.2023.2209115>.

© 2023 The Author(s). Published with license by Taylor & Francis Group, LLC.

This is an Open Access article distributed under the terms of the Creative Commons Attribution License (<http://creativecommons.org/licenses/by/4.0/>), which permits unrestricted use, distribution, and reproduction in any medium, provided the original work is properly cited. The terms on which this article has been published allow the posting of the Accepted Manuscript in a repository by the author(s) or with their consent.

2019). Mechanistic studies have for instance shown the impairment of the eye development and function, supported by the alteration of the retinoid signaling pathway (Bérubé et al. 2023; González-Penagos et al. 2022; Lie et al. 2019; Sørhus et al. 2021). A few studies have investigated the impact of crude oil on capelin early life stages. Based on these and their effect concentrations (expressed in terms of sum of PAHs), we hypothesize that capelin early life stages may be relatively robust to exposure to crude oil and associated mixtures compared to other fish species from both cold-water (Bender et al. 2021; Hansen et al. 2021; Nahrgang et al. 2016; Sørensen et al. 2017) and warm-water marine environments (reviewed by Pasparakis et al. 2019). Paine et al. (1992) showed a higher sensitivity to crude oil exposure in larval stages compared to embryonic stages of capelin. In 2012, Frantzen et al. showed developmental delays and increased embryonic mortality under exposure to a water-soluble fraction (WSF) of crude oil (initial sum of 26 PAHs above 40 µg/L). However, typical symptoms of yolk sac and pericardial edema, hemorrhages, and craniofacial abnormalities were not observed at the exposure concentrations used (Frantzen et al. 2012). Several studies have also investigated the impact of dispersed oil and dispersant (Beirão et al. 2019; Beirão, Litt, and Purchase 2018; Tairova et al. 2019). Capelin sperm fertilization ability was reduced under a dispersed oil exposure and attributed the effect to the dispersant rather than the crude oil (Beirão, Litt, and Purchase 2018). Chemically dispersed oil also led to dose-dependent reductions in hatching success, heart rates at sum of 18 PAHs down to 2.8 µg/L (Beirão et al. 2019), and an increased prevalence of larval deformities (craniofacial abnormalities, body axis defects, reduced total body length) were shown by Tairova et al. (2019) (sum of PAHs not known).

One major hindrance in comparing sensitivities across species and studies is the influence of the exposure designs including exposure regimes, crude oil fractions (dispersed, water-soluble, etc.), as well as the origin and composition of the crude oil. Therefore, the present study aimed at evaluating the sensitivity of beach-spawning capelin early life stage to crude oil WSF using the same exposure design, crude oil, and concentration range as previously used in our research group on polar cod

(*Boreogadus saida*) (Bender et al. 2021). Bender et al. (2021) showed dose-dependent increased mortality, prevalence of malformations, and reduced larval length in polar cod exposed throughout the embryo stage to a WSF of crude oil at initial levels of sum of 44 PAHs below 250 ng/L. This study reported some of the lowest effective concentrations found in the literature for fish early life stages exposure to crude oil and constitutes an interesting basis for comparison with the possibly more robust capelin. Capelin embryos collected on beaches of Northern Norway were exposed until hatch, similarly to Bender et al. (2021). Prevalence of malformations in embryos as well as larval mortality, cardiac activity, and length were recorded. We hypothesized that the early life stages of beach-spawning capelin exposed to a crude oil WSF would show similar effects to that observed in Bender et al. (2021) but at higher doses.

Material and methods

Ethical statement

The present experimental work was performed according to regulations enforced by the Norwegian Animal Research Authority (ID 19371).

Collection of the capelin eggs

On the 13th of April 2019, beached-spawned capelin eggs deposited on coarse sand were collected in Loddebukta, Balsfjorden (N 69°14', E19°13'). The eggs were kept in a cold and humid box for the 2-h transit to the research station of Akvaplan-niva at Kraknes. Upon arrival, the egg-bearing coarse sand was placed in a shallow tank receiving flow-through seawater (5 °C, 60 µm filtered and UV-treated).

Experimental design

Capelin embryos were exposed to crude oil WSFs using oiled gravel columns, as described by Bender et al. (2021). Briefly, gravel (7–9 mm) was rinsed with tap water, soaked in 1 M HCl for 2 h, rinsed, and left in 90% ethanol overnight. The following day, the gravel was rinsed again with tap water before it was dried at 60 °C for 10–12

h. The gravel was then coated in portions of 2 kg and hand shaken for 1 min, with crude oil (Kobbe oil from the Barents Sea shelf) at four different concentrations: Low (0.19 g oil/kg gravel), Medium (0.75 g oil/kg gravel), High (3 g oil/kg gravel), and Extra High (6 g oil/kg gravel). The control gravel was washed in the same way, but not coated with crude oil. After the coating, the gravel was air-dried for 3 d at ambient temperature (7 °C). The control treatment gravel was kept in separate rooms during drying to avoid cross-contamination. Five 1-m-high PVC columns were loaded with 11 kg of oiled or clean control gravel. The five columns were capped with Zoobest aquarium filter wool made from polyester fibers to reduce the presence of oil droplets from entering the effluent water. Each column was flushed for 70 h with filtered (60 µm) and UV-treated seawater at a flow rate of 80 L/h per column. The flushing and drying of the columns aimed to remove the highly volatile and acutely toxic BTEX (benzene, toluene, ethylbenzene, and xylene) compounds before the exposure start and achieve the initial PAH aqueous concentrations in the lower µg/L range. The columns were prepared 3 d in advance of the experiment, drained from the remaining water, and frozen at -20 °C after initial flushing.

Exposure of capelin embryos to the water-soluble fraction (WSF) of crude oil

On the day of the exposure start, each gravel column was thawed in the experimental room for 2 h. The water flow was then started 2 h prior to the transfer of egg-bearing substrate to each incubator. The concentration of eggs per gram of substrate (coarse sand) was estimated on four sub-samples. The egg-bearing substrate was then distributed to the 20 experimental incubators aiming to achieve approximately 8,000 eggs per incubator, equaling about 200 g of coarse sand substrate. Embryos were studied under a stereomicroscope and estimated to be 6 d post fertilization (dpf) at the beginning of the experiment, corresponding to the crack of the optic bulb developmental stage, just before the end of organogenesis I (Fridgeirsson 1976) (Figure S1). The entire egg-bearing substrate layer was laying on a fine mesh netting, elevated from the bottom of the incubator to allow a homogenous exposure of the entire substrate and a better gas exchange

within the incubator. At the exposure start, the columns were connected to four 2 L incubators, providing a continuous upward flow (20 L/h) of filtered and UV-treated seawater. The entire setup consisted thus of 20 incubators (5 treatments × 4 replicates) (Figure S2A).

The water temperature (5.5 ± 0.3 °C throughout exposure and 5.3 ± 0.6 °C throughout the post-exposure period) was monitored using three Onset UA-002-64 HOBO Pendant®, and light conditions were set to constant dimmed light.

End of exposure and hatching

After 19 d of exposure (25 dpf), 3 d prior to the onset of hatching, exposure was stopped. Each of the 20 incubators containing egg-bearing substrates were placed in 25 L conical tanks to allow for optimal swimming and growth conditions of hatched larvae (Figure S2B). The incubators received a continuous flow of clean filtered seawater (60 µm, UV-treated, 25 L/h) until the end of the experiment (46 d of experiment, 52 dpf). The 25 L tanks were aerated with 3 cm cylindrical air stones to ensure that the larvae and feed particles (section 2.3.3) did not adhere to the water surface and were mixed throughout the water column.

The first observation of hatched larvae occurred at 28 dpf. Hatching was further stimulated at 31 dpf by gentle shaking of the 2 L incubators to assist larvae possibly stuck in the gravel to pass over to the larger tanks. The end of the hatching was marked at 36 dpf, and the 2 L incubators were removed from the 25 L tanks. Larvae remained in the 25 L tanks from where all further sampling was executed until the end of the experiment at 52 dpf. Figure 1 provides a timeline of the capelin experiment with exposure start and end, as well as a sampling timeline.

Larvae feeding regime

Feeding of larvae was initiated at 30 dpf, 2 d after the beginning of hatching. Live rotifer cultures produced by Nofima AS were mixed with green algae, *Nannochloropsis* (Nanno 3600, Reed Mariculture) to create a visual contrast for the food in the water column and thereby increase larval feeding success (Stuart and Drawbridge 2011). The larvae were fed live rotifers and algae

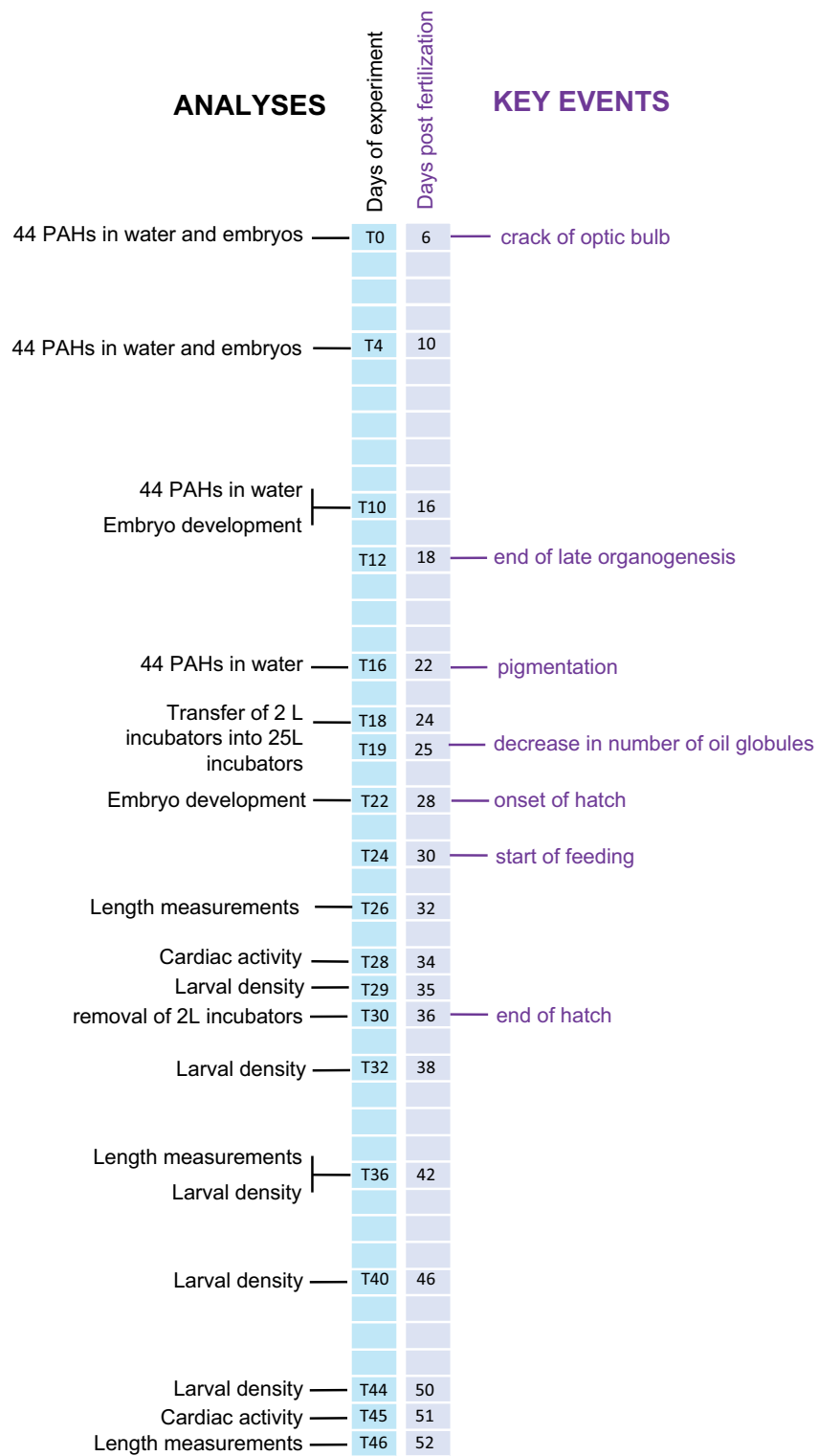


Figure 1. Timeline of the experiment. Left-hand axis represents the days of experiment (T) with key experimental and sampling events annotated (black font); right-hand axis represents the age of the capelin early life stages in days post fertilization (dpf), with key embryo developmental stages (violet font).

mixture (75,000–125,000 rotifers per incubator) three or four times a day until 51 dpf.

Sampling and data analysis

Chemistry sampling and analysis

Water samples (1 L in duplicates per treatment column) were taken directly from the outlet of each oiled gravel column at the start of the exposure and after 4, 10, and 18 d of exposure, corresponding to embryos of age 6, 10, 16, and 24 dpf ($n = 40$ samples). The samples were frozen ($-20\text{ }^{\circ}\text{C}$) in amber glass bottles. Prior to the analysis, samples were carefully thawed at $4\text{ }^{\circ}\text{C}$, acidified (15 % HCl), and stored in a dark and cool ($4\text{ }^{\circ}\text{C}$) environment until extraction. One of each duplicate sample for each treatment and timepoint taken ($n = 20$) was extracted and analyzed according to Bender et al. (2021).

Embryos attached to the substrate ($n = 155 \pm 53$) were sampled 4 d into the exposure (10 dpf) from each incubator and frozen at $-80\text{ }^{\circ}\text{C}$. Prior to shipment, frozen batches of eggs were transferred to individual petri dishes and soaked in 5 mL KOH solution 2 % (m/v) for 2 h to separate adherent eggs from the coarse sand as much as possible. After separation, eggs were accurately counted and coarse sand removed, before being placed back into cryotubes and refrozen at $-80\text{ }^{\circ}\text{C}$ until analysis.

Embryo samples were extracted without weighing due to coarse sand residues. Extraction was otherwise performed as described in Sørensen et al. (2016).

For quantification of 44 PAHs, extracts of eggs and water were analyzed by an Agilent 7890 gas chromatograph coupled with an Agilent 7010B triple quadrupole mass spectrometer fitted with an EI source and collision cell was used (Agilent Technologies, Santa Clara, CA, USA). To Agilent J&W HP-5 MS UI GC-columns ($30\text{ m} \times 0.25\text{ mm} \times 0.25\text{ }\mu\text{m}$) were coupled in series through a purged ultimate union (PUU). The carrier gas was high-purity helium at constant flow (1.2 mL/min). Samples ($1\text{ }\mu\text{L}$) were injected at $310\text{ }^{\circ}\text{C}$ splitless. The oven temperature was kept at $40\text{ }^{\circ}\text{C}$ for 1 min, then ramped to $110\text{ }^{\circ}\text{C}$ by $40\text{ }^{\circ}\text{C/min}$, to $220\text{ }^{\circ}\text{C}$ by $6\text{ }^{\circ}\text{C/min}$ and finally to $325\text{ }^{\circ}\text{C}$ by $4\text{ }^{\circ}\text{C/min}$. The temperature was then held at $330\text{ }^{\circ}\text{C}$ for 5 min, while the first column was back-flushed. The transfer-line temperature was $300\text{ }^{\circ}\text{C}$, the ion source temperature was $230\text{ }^{\circ}\text{C}$, and the quadrupole temperatures

were $150\text{ }^{\circ}\text{C}$. The EI source was operated at 70 eV. N_2 was used as collision gas at a flow of 1.5 mL/min and helium was used as a quenched gas at a flow of 2.25 mL/min . Target PAH analytes were identified by two unique MRM transitions and quantified by the most intense peak (Sørensen et al. 2016). Alkyl PAH clusters were determined by MRM using transitions from the molecular ion, as described previously in Sørensen, Meier, and Mjøs (2016). Standards were run throughout the sample sequence to monitor the system performance, and a variation of no more than 25 % was accepted. Parent PAH compounds were quantified by quadratic regression of a 12-level calibration curve ($0.01\text{--}100\text{ ng/mL}$), while alkyl PAH homologue groups were quantified by the response factor calculated for a methyl-substituted PAH reference compound ($2.5\text{--}100\text{ ng/mL}$). For the data treatment, individual PAH concentrations below the level of detection (LOD) were set to zero. A list of 44 analytes, their LODs, and all measured PAH concentrations in the water and embryo samples are published in the DataverseNO data repository (<https://doi.org/10.18710/CHHSXW>).

Embryo development and larval mortality

The proportion of abnormally developed embryos was determined during the exposure period at 16 dpf and at 28 dpf corresponding to late organogenesis and the onset of hatching, respectively. A subsample of egg-bearing substrates was taken from each incubator and distributed in a Bogorov counting chamber. Using a Leica M205 C stereomicroscope with a camera (Leica, MC 170 HD), the embryos ($n = 48 \pm 20$ eggs per incubator) were classified as normal or abnormally developed based on overall assessment of eye pigmentation, oil globules in the yolk sac and embryo size within the egg. The eggs used for the sampling were discarded after the counting. Counts of dead eggs were not considered due to the unknown decomposition rate and disappearance of egg remains from the coarse sand.

The high density and homogenous distribution of free-swimming larvae in the entire water column impeded tapping the bottom of the incubators for counting of dead larvae sinking to the bottom of the tanks. Instead, the density of free-swimming larvae was determined at 35, 38, 42, 46, and 50

dpf. A time-dependent decrease in larval density provided an indirect measure of larval mortality. Prior to the larval density sampling, the aeration strength was increased to homogenize the larval distribution and optimize sampling precision. Three subsamples of 100 mL were collected from the well-homogenized water column of each tank, using a plastic tube inserted vertically through the entire water column height of the 25 L tank. The larval density (larvae per liter) for each incubator was estimated from the average count of the three sub-samples. Density data for each incubator over time are presented as the mean of the three sub-samples, normalized to the first density count (35 dpf) of each respective incubator.

Larval length at age

Larval length was measured at 32, 42, and 52 dpf. Briefly, aeration in the tanks was lowered, and 30 larvae were sampled from the incubator surface. Only larvae that were seemingly in good condition by visual assessment (i.e., swimming actively and normally pigmented) were picked using a plastic pipette. The larvae ($n = 30$ per incubator) were placed onto a watch glass ($n = 5$ per glass) containing a drop of carbonated water to anesthetize the larvae during the procedure and photographed using a Leica M205 C stereomicroscope with a camera (Leica, MC 170 HD). All pictures were visually assessed to identify potential malformations (i.e., craniofacial deformities and body axis defects) and analyzed using the open-source software ImageJ (1.52q) to measure the larvae length (measurement made to the nearest 0.001 mm).

Cardiac activity

Video recordings of heart rate (beats per minute) and arrhythmia analyses were conducted on larvae after 34 and 51 dpf (28 and 45 d of experiment) using a Leica M205 C stereomicroscope with a Leica MC 170 HD camera connected to the Leica Application Suite. A temperature-controlled microscope stage was used to ensure that larvae were kept at a constant low temperature (5 °C) during the recording to minimize the potential effect of temperature stress on the heart. Larvae that were seemingly in good condition were picked from the 25 L incubators using a pipette and allowed to acclimatize on the

cooling stage in a watch glass containing methylcellulose (3% in seawater) for a few minutes before the recording started. In total, 20 larvae from each treatment ($n = 5$ per replicate incubator) were sampled and recorded for at least 1 min. The heart rate (beats per minute) was determined by counting heartbeats from 20–30-s video segments. Cardiac arrhythmia was assessed on the Control and Extra High treatment at 51 dpf only ($n = 20$ per treatment), by determining the inter-beat variation from the same video segments as for the heart rate, according to Incardona et al. (2009). The videos were analyzed using VLC media player (Version 3.0.8 Vetinari).

Statistical analyses

All experimental data were analyzed with R version 4.2.1 (R Core Team 2022). For visualizing only a few data points, dot plots of the values were made, whereas for larger sets of values boxplots were used (Greenacre 2016). Density and length measurements were log-transformed for statistical analyses. A linear mixed effect (lme) model using the “Nonlinear Mixed Effects Models” package nlme (Pinheiro et al. 2023) evaluated the length and density data with treatment and time as fixed factors and incubators as a random factor, followed by estimated marginal means (EMMs), also known as least-squares means, with Tukey correction of p-values as a post hoc multiple comparison model. For heart rate and arrhythmia, normal distribution of residuals was assessed using a Shapiro–Wilk test, and visual assessment of the Q–Q plot supported the test. If normality requirements were met (arrhythmia), a one-way analysis of variance (ANOVA) with a subsequent Tukey HSD post hoc test on differences between means was followed. If normality requirements were not met (heart rate), a non-parametric Kruskal–Wallis test, followed by a post hoc Dunn test, was performed with Hommel false discovery rate (FDR) corrections of the p-values. A similar approach using the Kruskal–Wallis test for non-normal data was used to ascertain if there were significant differences between treatments regarding the proportions of abnormal embryos. For all analyses, the threshold for the statistical significance level was set to $\alpha = 0.05$.

Results

Chemistry analyses

Water samples from the crude oil experiment taken at days 0, 4, 10, and 18 were analyzed for 44 parent and alkylated PAHs. The initial sum of 44 PAH concentrations in the water was 19.25-, 9.36-, 1.95-, 0.53-, and 0.072 $\mu\text{g/L}$ for Extra High, High, Medium, Low, and Control, respectively (Figure 2a). As expected, the highest concentration of the sum of 44 PAHs was measured at the start of the experiment (embryos aged 6 dpf) and declined between 85 % and 94 % over the 18 d of exposure period for all treatments, reaching 2.15 $\mu\text{g/L}$, 0.56 $\mu\text{g/L}$, 0.13 $\mu\text{g/L}$, and 0.08 $\mu\text{g/L}$ for treatments Extra High, High, Medium, Low, and Control, respectively.

The relative abundance of the 44 PAH compounds analyzed in the WSF of crude oil changed throughout the exposure period with smaller and less substituted PAHs predominating at the start of the experiment (Figure S3). At the start of the experiment, naphthalene and its alkylated homologs amounted for 76–80% of the total dissolved sum of 44 PAHs in the High and Extra High treatment, while their relative proportion decreased with treatment (59 % and 25 % in medium and low, respectively). During the sampling period (0–18 d of exposure), the proportion of unsubstituted naphthalenes consistently declined

over time, primarily for the less substituted homologs (C1 – C3). The relative abundance of the more substituted naphthalene homolog C4 increased until 10 d of exposure. Phenanthrenes and fluorenes were the second and third most dominant groups of aqueous PAHs analyzed. Their relative proportion increased with treatment at the exposure start (from 17% tricyclic aromatic hydrocarbons in the Extra High to 62 % in the Low treatment) and represented between 29 % and 39 % of sum 44PAHs after 18 d of experiment. After 4 d of exposure, embryos had accumulated PAHs dose-dependently (Figure 2b). Levels of 44 PAHs ranged between 0.24 ± 0.08 ng/egg (Low) and 10.58 ± 0.89 ng/egg (Extra High) in the treatment groups compared to Control (0.05 ± 0.01 ng/eggs). Similar to the aqueous composition, naphthalenes dominated the body burden profiles (28–53 %), followed by the phenanthrenes (12–33 %) and the fluorenes (6–8 %) (Figure 3).

Embryo development and larval mortality

The proportion of abnormally developed embryos did not show any clear dose-dependent effects at 16 and 28 dpf (Figure 4). At 16 dpf (10 d of experiment), the mean proportion of abnormal embryos was below 4 % across treatments (from 1.18 % in the Medium group to 3.58 % in the Control group). At 28 dpf (22 d of experiment), the mean proportion of abnormally

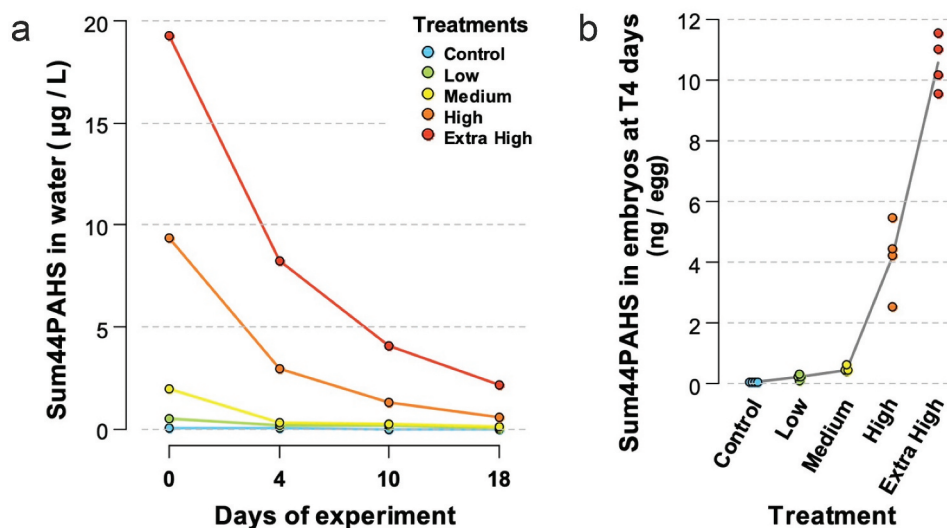


Figure 2. (a) Sum of 44 PAHs ($\mu\text{g/L}$) in the effluent water from the gravel columns (no replication) at 0, 4, 10, and 18 d of exposure, corresponding to embryos at 6, 10, 16, and 24 dpf, respectively. (b) Sum of 44 PAHs (ng/egg) accumulated in 10 dpf embryos after 4 d of exposure. Dots represent incubator-specific levels, and the line connects the overall means.

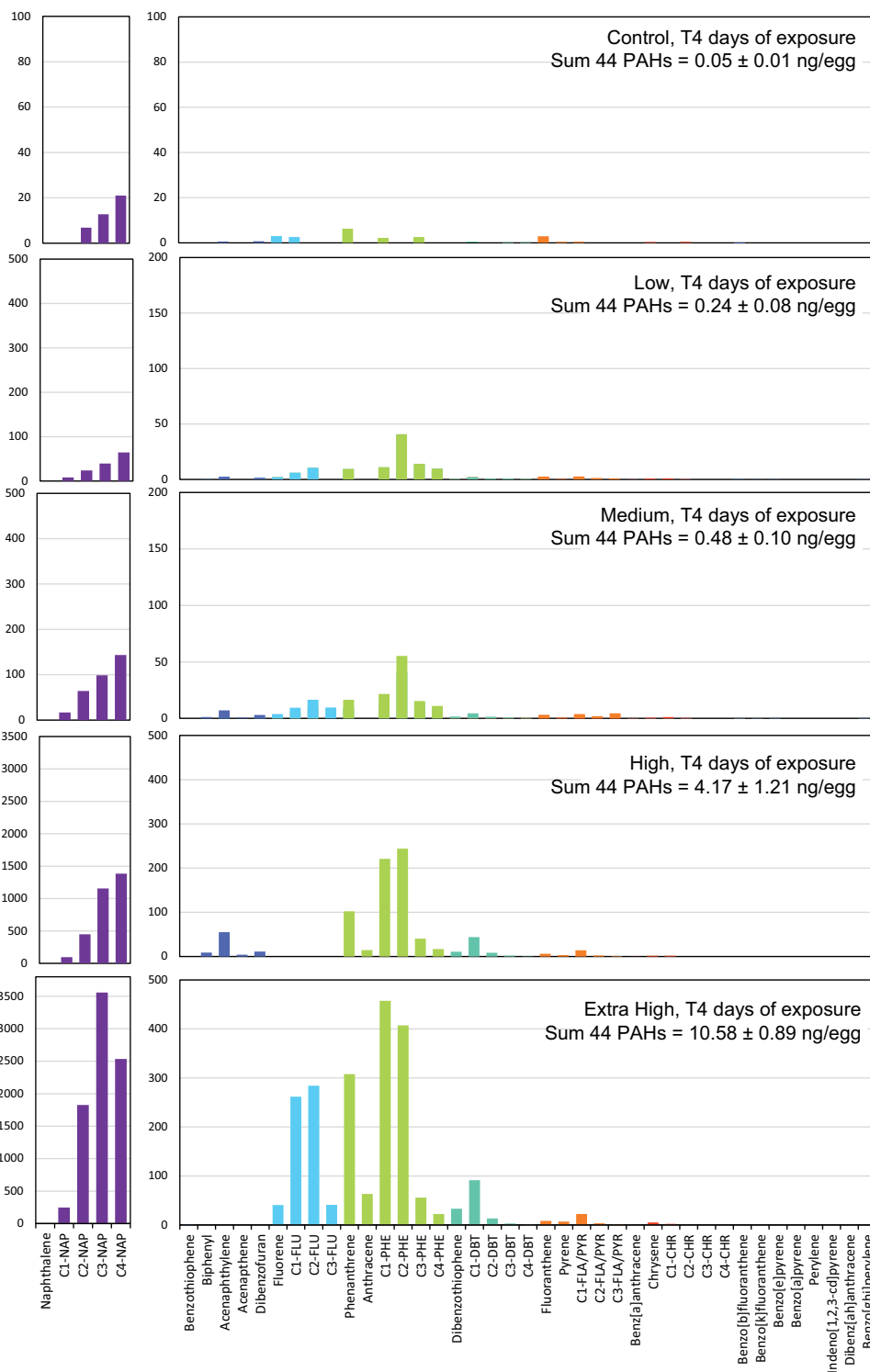


Figure 3. Concentration of 44 PAHs (pg/egg) in embryos of the Control, Low, Medium, High, and Extra High groups following 4 d of exposure. The sum of 44 PAH concentrations (ng/egg wet weight) is listed for each treatment group. Parent compounds are indicated with full name, while alkylated homologs are indicated as C1-, C2-, C3-, and C4-.

developed embryos had increased but remained below 8% in all treatments (range from 0.40 % in the Extra High group to 7.85 % in the High group). The only Control – oil-exposed treatment difference

that was individually significant was for the High group ($p = 0.02$), although the significance at the 0.05 level is not accepted when the FDR adjustment is made.

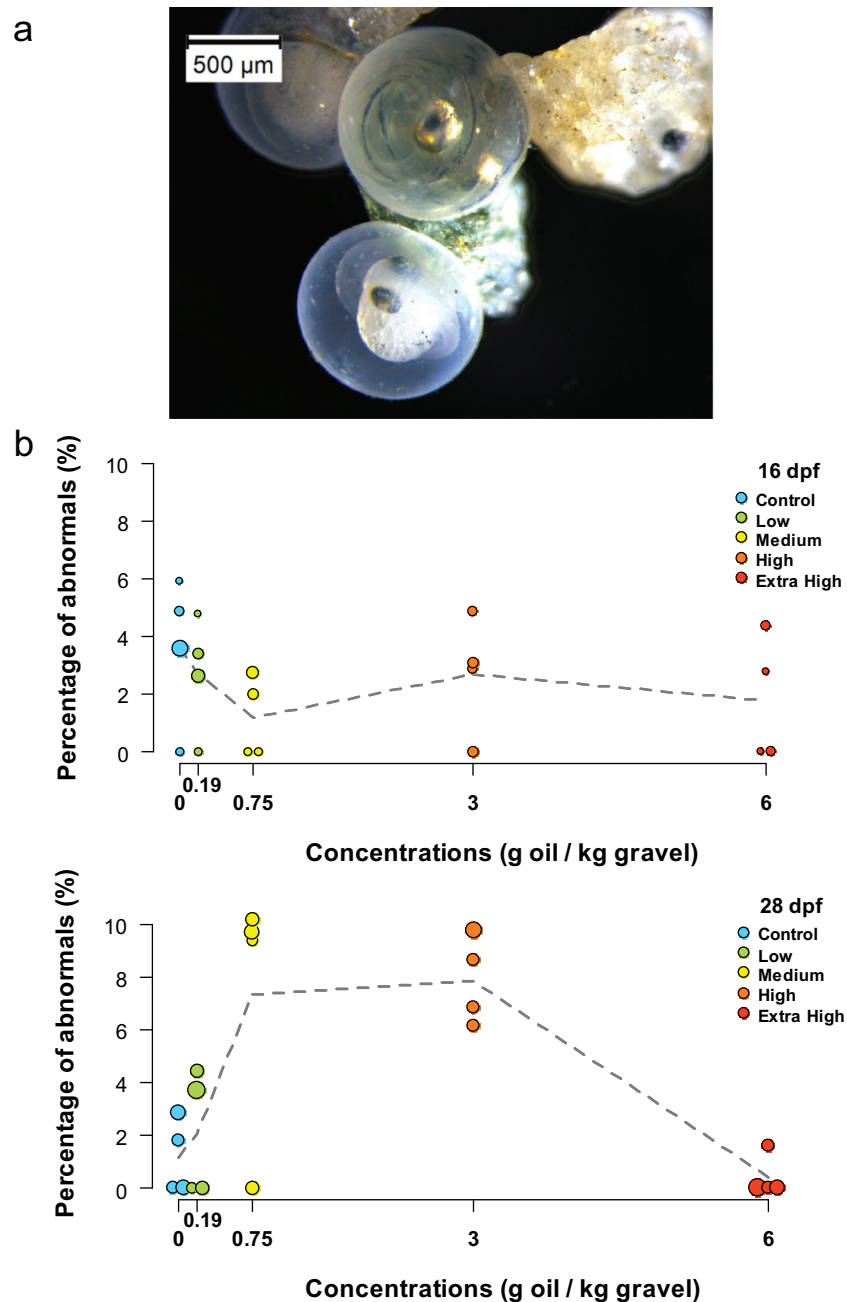


Figure 4. (a) Representative photograph of a normally (top) and abnormally (bottom) developed embryo at 28 dpf. (b) Percentage abnormally developed embryos at 16 dpf and 28 dpf, corresponding to 10 and 22 d of experiment. The means of the four incubators for each treatment are plotted as dots and the dashed line connects the overall means. $n = 48 \pm 20$ larvae were assessed per incubator. The size of the dots is proportional to the specific n per incubator (range 17–82, and 35–97 eggs counted per incubator at 16 and 28 dpf, respectively).

Following peak hatch at 35 dpf (29 d of experiment), the initial larval density was significantly higher in the low incubators (range 168–220 larvae/L, $p < 0.001$) and Extra High incubators (range 157–366 larvae/L, $p < 0.01$) compared to the controls (range 55–103 larvae/L). In general, there was also large variability in larval densities between incubator replicates

throughout the experiment, especially one replicate incubator in the Extra High group that showed very high average densities (Figure S4). All treatment groups decreased in larval density (44–61%) between 35 dpf and 50 dpf, but there were no significant differences in the decrease in density between treatment groups (Figure 5). Mean larval densities at 50 dpf ranged from

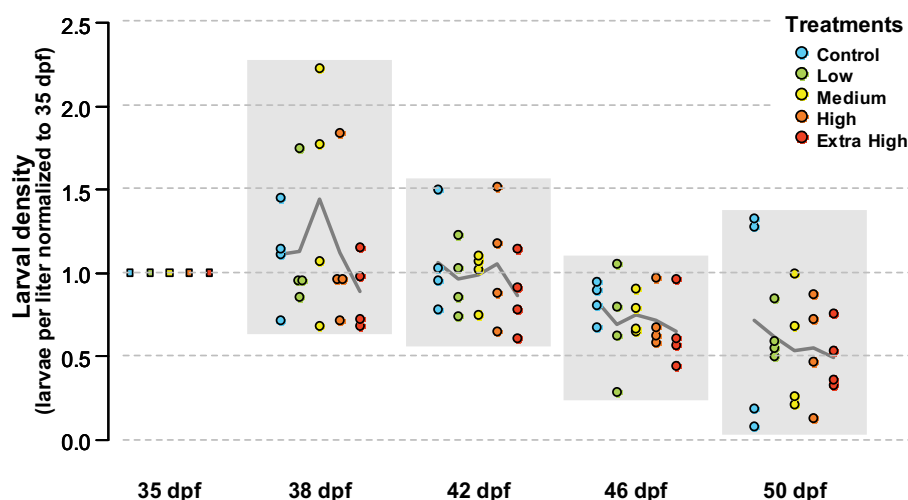


Figure 5. Larval density (larvae per liter) from 35 dpf until 50 dpf, corresponding to 29–44 d of experiment. The means of the four incubators for each treatment, normalized to incubator-specific densities at 35 dpf, are plotted as dots, and the line connects the overall means.

120 larvae/L (Extra High) to 38 larvae/L (Medium).

Larval length at age

There were no significant differences in larval length across treatments for any of the measured timepoints (Figure 6). The mean (\pm SD) larval length at 32 dpf was between 6.5 ± 0.3 mm (Control, Medium, and High) and 6.7 ± 0.3 mm (Low). At 42 dpf, all treatments showed an increase in mean length between 6.9 ± 0.4 mm (Extra High) and 7.2 ± 0.5 mm (Low). Finally, at 52 dpf, average larval length in the

treatments ranged between 7.0 ± 0.5 mm (Medium and High groups) and 7.1 ± 0.5 mm (Control and Extra High). Visual assessment of larvae pictures did not reveal any malformations.

Cardiac activity and arrhythmia in larvae

Larvae collected from the water column at age 34 and 51 dpf, corresponding to 28 and 45 d of experiment, did not show significant differences in heart rate between treatment replicates or across treatments (Figure 7a). At 34 dpf, the mean (\pm SD) heart rates of the larvae were 58 ± 23 , 57 ± 26 , 50 ± 22 , 50 ± 22 ,

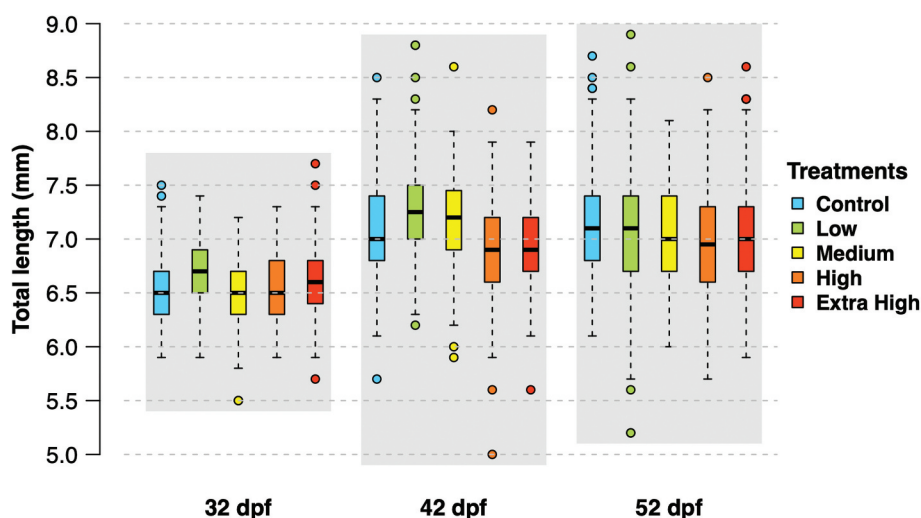


Figure 6. Length (in mm) of larvae ($n > 114$ per treatment) sampled at 32, 42 and 52 dpf, corresponding to 26, 36 and 46 d of experiment. Box plots represent the median (line), 25–75% percentiles (box), non-outlier range (whisker), and outliers (circles).

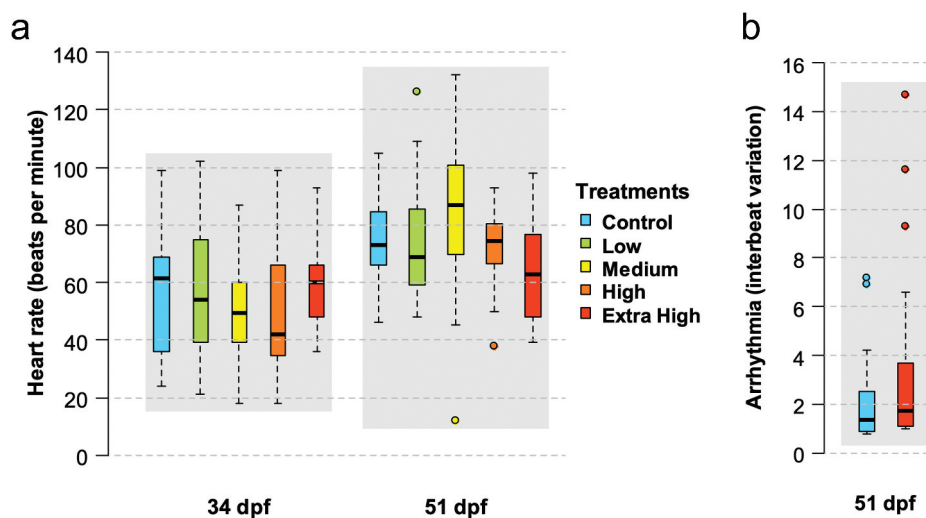


Figure 7. (a) Cardiac activity (heart rate in beats per minute) measured on larvae ($n=20$ per treatment) at 34 and 51 dpf. (b) Arrhythmia (interbeat variation) measured on larvae ($n=20$ per treatment) in the Control and Extra High treatment groups. Box plots represent the median (line), 25–75% percentiles (box), non-outlier range (whisker) and outliers (circles).

and 58 ± 16 beats per minute in the Control, Low, Medium, High, and Extra High treatments, respectively. At 51 dpf, the heart rate of the larvae increased on average compared to 34 dpf larvae, ranging between 63 ± 18 beats per minute (Extra High) and 85 ± 28 beats per minute (Medium).

Arrhythmia measured as inter-beat variation showed no significant differences ($p = 0.284$) between the Control (2.34 ± 2.17) and Extra High (3.67 ± 4.12) treatments at 51 dpf (Figure 7b). No further examinations were conducted on the remaining treatments and timepoints. Additionally, no malformations (i.e., craniofacial abnormalities or body axis defects) were observed by visual assessment in any of the hatched larvae assessed for cardiotoxicity (not shown).

Discussion

Exposure of capelin to a crude oil WSF during the embryonic development phase (6 dpf to 24 dpf) did not lead to embryo malformations, larval mortality, alterations in larval length, and heart rate in larvae (compared to controls). Initial PAH waterborne concentrations were in the lower $\mu\text{g/L}$ range and decreased rapidly over time, corresponding to environmentally realistic levels found in post-spill seawater samples (Boehm et al. 2007; Sammarco et al. 2013). These PAH concentrations were also

comparable to other experimental studies on capelin early life stages exposed to water accommodated fractions of crude oil (Beirão et al. 2019; Beirão, Litt, and Purchase 2018) and experiments employing similar oiled-gravel column exposure designs (Bender et al. 2021; Frantzen et al. 2012). The present highest crude oil concentrations used to coat the gravels (3 and 6 g oil/kg gravel in High and Extra High, respectively) corresponded to the low and medium oil concentrations in Frantzen et al. (2012) respectively. Initial total aqueous PAH concentrations in our High (3 g oil/kg gravel) treatment ($9.36 \mu\text{g/L}$) were similar to the corresponding treatment ($14.6 \mu\text{g/L}$) in Frantzen et al. (2012); however, our Extra High treatment ($19.25 \mu\text{g/L}$) was notably lower than the corresponding treatment ($40.4 \mu\text{g/L}$) in Frantzen et al. (2012). This could be related to different flushing times of the columns (70 h in this study compared to 48 h in Frantzen et al. (2012)) as well as other factors (e.g., gravel size, drying time, and water flow rate). In another study using the same experimental setup, crude oil, and concentration range (0.19–3 g oil/kg gravel) to expose polar cod at two different temperatures (0.5 and 2.8 °C), Bender et al. (2021) reported initial aqueous PAH levels almost two orders of magnitude lower (140 ng/L and 237 ng/L compared to $9.36 \mu\text{g/L}$ in the High treatment of the present study, respectively). Slight differences

in flushing time, water flow rate, and especially seawater temperature may have significantly affected the waterborne concentrations of petroleum compounds over time. Temperature also affects the composition of the WSF, with the presence of bulk oil reported in the 2.8 °C group compared to the 0.5 °C in Bender et al. (2021). Although not analyzed in the present study, it is possible that the exposure also contained some bulk oil or oil droplets.

Assuming capelin eggs of 1 mm in diameter correspond to 1 mg of wet weight (Lønning et al. 1988) the highest measured PAH levels in capelin following 4 d of exposure were approximately 10,000 ng/g embryo wet weight in the highest treatment (measured: 10.58 ng/egg wet weight, Extra High). These levels were significantly higher than polar cod embryos of the same treatment and exposure time in Bender et al. (2021). But, considering comparable initial aqueous PAH levels (237 and 527 ng/L in polar cod and capelin exposure water, respectively), the concentration bioaccumulated for polar cod (843 ng/g at 2.8 °C) was four times higher than that for capelin (236 ng/g at 5.5 °C). Despite high accumulated PAH concentrations in capelin eggs (up to 10,000 ng/g), no significant effects in terms of larval mortality, malformations, length at age, and cardiac activity were observed. It is noteworthy that a fraction of the PAHs quantified in the eggs may be adsorbed to the eggs, as opposed to absorbed, and thus that the actual bioaccumulated fraction in the embryonic body may be lower than reported in our PAH analysis (Sørhus et al. 2015). Capelin has a thick double-layered chorion (Lønning 1981) that may be resistant to contaminant uptake. Future studies should consider analyzing the bioaccumulated fraction on dechorionated eggs, as well as include the analysis of phase I cytochrome P450 induction as a biomarker of exposure. Nevertheless, in comparison, polar cod showed significant effects in the highest treatments, with PAH levels between 400 and 800 ng/g embryo wet weight after 4 d exposure (Bender et al. 2021). In a similar oiled gravel column setup, pink salmon (*Oncorhynchus gorbuscha*) also showed significant cardiotoxicity when exposed to an initial waterborne PAH concentration of 15.4 µg/L, corresponding to 634 ng/g embryo wwt (Incardona et al. 2015). Our findings

support previous studies (Beirão et al. 2019; Beirão, Litt, and Purchase 2018; Frantzen et al. 2012) that did not find significant effects in crude oil-exposed capelin embryos with initial aqueous PAH concentrations below about 40 µg/L (Beirão et al. 2019; Frantzen et al. 2012) and bioaccumulated levels below 10,000 ng/g embryo (this study). Under the fragile assumption that bioaccumulated PAH concentrations in embryos can be used as an exposure proxy for complex crude oil mixtures and lacking better comparative means, our findings suggest that capelin early life stages are less sensitive to crude oil WSF than other species at comparable levels of exposure and bioaccumulated PAH concentrations (reviewed by Pasparakis et al. 2019). A more exhaustive chemical characterization of our exposure water would however be necessary to provide a more reliable conclusion. A large number of unresolved compounds, such as monoaromatic petroleum hydrocarbons, are present in the WSF and shown to be potentially bioavailable and toxic to aquatic organisms (Booth et al. 2008; Melbye et al. 2009; Petersen et al. 2017; Sørensen et al. 2019). The measure of 44 PAHs alone provides a weak basis for comparing embryotoxicity from the complex WSF (Hansen et al. 2019; Meador and Nahrgang 2019).

We failed to detect any cardiac impairments, malformations, or length differences in the hatched larvae from any treatments. Heart rates of capelin larvae were in the same range as control levels reported elsewhere (Beirão et al. 2019). Frantzen et al. (2012) and Paine et al. (1992) also failed to detect developmental deformities in capelin larvae exposed to crude oil even at higher aqueous PAH concentrations. In contrast, Tairova et al. (2019) reported significant and dose-dependent deformities in capelin larvae exposed to water accommodated fraction (WAF) and chemically enhanced WAF. Unfortunately, exposure metrics were expressed only as nominal total hydrocarbon content (THC) and could not be directly compared to the present study. The lack of observed larval deformities in this study may be linked to the lack of cardiac impairment as developmental effects in the form of body fluid accumulation, craniofacial, and body defects are suggested to be secondary to reduced cardiac function (Esbaugh et al. 2016;

Incardona and Scholz 2016; Incardona et al. 2014). Sampling of larvae for heart rate analysis, as well as morphometric analyses, were biased toward freely-swimming larvae in the top layers of the incubators. Thus, the most weakened and malformed individuals that would sink to the bottom of the incubators were missed. Nevertheless, Nahrgang et al. (2016) showed an increasing degree of malformations with dose visible also in surface-swimming polar cod larvae, and a dose-dependent decrease in length in organisms with no visible malformations. Here, no indications of adverse effects or a dose-dependent decrease in larval density over time were observed for capelin larvae.

Heart malformations and deformities at the embryonic stage are frequently associated with increased embryo mortality and lower hatching rates (Hansen et al. 2021; Nahrgang et al. 2016; Sørensen et al. 2017). Embryos sampled at 16 and 28 dpf did not show any dose-dependent malformation, and the frequency of occurrence of malformations coincided well with levels reported in unexposed capelin embryos (below 10% at 5 °C, Shadrin, Makhotin, and Eriksen 2020). The large variability in larval density at hatch among incubators likely reflected an uneven distribution of eggs due to a patchy distribution of fertilized eggs on the substrate. Nevertheless, the high larval density in all treatments at hatch did not suggest any dose-related mortality occurring during the embryonic phase.

The lack of effects seen in crude oil-exposed capelin at exposure levels that lead to developmental impairment in other fish early life stages could be attributed to an exposure outside of a developmentally sensitive time-window (i.e., “teratogenic window”), and an intrinsic robustness of the capelin species’ attributable to evolutionary mechanisms. The timing of exposure relative to the developmental stage may be critical in determining the extent of developmental effects in fish embryos (Beirão et al. 2019; Bérubé et al. 2023; McIntosh et al. 2010; Paine et al. 1992; Perrichon et al. 2021; Sørhus et al. 2021). Beirão et al. (2019) found lower embryotoxicity of crude oil to capelin exposed from 6 dpf to hatching compared to 0 dpf to hatching. Our embryos were estimated to be 6 dpf at the onset of exposure, corresponding to the formation of pre-

organs (organogenesis I, Fridgeirsson 1976), suggesting that the most critical exposure window was avoided in the present study. However, in Frantzen et al. (2012) capelin exposed from the end of gastrulation, an earlier developmental stage, did not show developmental effects when exposed to higher levels than in this study. Thus, the exposure window does not seem to be the main reason for a lack of biological effects in the present study. Tolerance to chemical exposure is in part determined by the species’ genome resources along with physiological traits, all affecting toxicokinetic and toxicodynamic traits (Spurgeon et al. 2020). For instance, species-specific differences in the numbers and composition of genes of the chemical defenseome (Goldstone et al. 2006) were found in five teleost species (Eide et al. 2021). These may play an important role in the species’ specific sensitivity to environmental stressors, including chemicals. Capelin eggs have been shown to be resistant to various environmental factors such as salinity and low temperatures (Davenport and Stene 1986; Davenport, Vahl, and Lønning 1979; Præbel, Christiansen, and Fevolden 2009). These embryo adaptations do not seem to be specific to the beach-spawning population but are also found in the offshore demersal Barents Sea population (Præbel et al. 2013), although local populations show differing genetic signatures with different spawning modes (Cayuela et al. 2020). There are currently no studies that have investigated the genomic resource underlying the tolerance of capelin to xenobiotics through, for instance, whole-genome mapping or comparative transcriptome analyses such as done for five other teleost species (Eide et al. 2021). The suggested high tolerance of capelin embryos to crude oil exposure could be linked to evolutionary developed physiological adaptations to various environmental pressures, including chemical pollution, and deserves further investigations.

Acknowledgments

The authors would like to acknowledge internship student Juliette Lavarec, the staff at the research station of Akvaplan-niva (Thor Arne Hangstad, Lauri Kapari,

Armand Nes, William Kristiansen, Ellie Watts), the rotifer culturists at Nofima, and laboratory staff at SINTEF Ocean (Marianne Rønsberg, Kjersti Almås, and Marianne Molid).

This work was supported by the Research Council of Norway under Grant 280724 (Arctic Ecosens) and under Grant 228107 (ARCEX), and the Fram Centre under Grant given to the project Cumulative Impact of Multiple Stressors in High North ecosystems (CLEAN).






Disclosure statement

No potential conflict of interest was reported by the author(s).

Funding

The work was supported by the Framcenteret [CLEAN]; Norges Forskningsråd [228107].

ORCID

Jasmine Nahrgang  <http://orcid.org/0000-0002-4202-5922>
 Cassandra Granlund  <http://orcid.org/0009-0004-7058-5857>
 Morgan Lizabeth Bender  <http://orcid.org/0000-0002-7301-613X>
 Lisbet Sørensen  <http://orcid.org/0000-0003-0455-3545>
 Michael Greenacre  <http://orcid.org/0000-0002-0054-3131>
 Marianne Frantzen  <http://orcid.org/0000-0003-4249-3360>

Data availability statement

The data that support the findings of this study are available in DataverseNO with the DOI identifier <https://doi.org/10.18710/CHHSXW>.

References

- Beirão, J., L. Baillon, M. A. Litt, V. S. Langlois, and C. F. Purchase. 2019. Impact of crude oil and the dispersant CorexitTM EC9500A on capelin (*Mallotus villosus*) embryo development. *Mar. Environ. Res.* 147:90–100. doi:10.1016/j.marenvres.2019.04.004.
- Beirão, J., M. A. Litt, and C. F. Purchase. 2018. Chemically-dispersed crude oil and dispersant affects sperm fertilizing ability, but not sperm swimming behaviour in capelin (*Mallotus villosus*). *Environ. Pollut.* 241:521–28. doi:10.1016/j.envpol.2018.05.080.
- Bender, M. L., J. Giebichenstein, R. N. Teisrud, J. Laurent, M. Frantzen, J. P. Meador, L. Sørensen, B. H. Hansen, H. C. Reinardy, B. Laurel, et al. 2021. Combined effects of crude oil exposure and warming on eggs and larvae of an arctic forage fish. *Sci. Rep* 11:8410. doi:10.1038/s41598-021-87932-2.
- Bérubé, R., C. Garnier, M. Lefebvre-Raine, C. Gauthier, N. Bergeron, G. Triffault-Bouchet, V. S. Langlois, and P. Couture. 2023. Early developmental toxicity of Atlantic salmon exposed to conventional and unconventional oils. *Ecotox. Environ. Safe* 250:114487. doi:10.1016/j.ecoenv.2022.114487.
- Boehm, P. D., J. M. Neff, and D. S. Page. 2007. Assessment of polycyclic aromatic hydrocarbon exposure in the waters of Prince William Sound after the Exxon Valdez oil spill: 1989–2005. *Mar. Pollut. Bull.* 54:339–56. doi:10.1016/j.marpolbul.2006.11.025.
- Booth, A. M., A. G. Scarlett, C. A. Lewis, S. T. Belt, and S. J. Rowland. 2008. Unresolved Complex Mixtures (UCMs) of aromatic hydrocarbons: Branched alkyl indanes and branched alkyl tetralins are present in UCMs and accumulated by and toxic to, the mussel *Mytilus edulis*. *Environ. Sci & Technol* 42:8122–26. doi:10.1021/es801601x.
- Cayuela, H., Q. Rougemont, M. Laporte, C. Mérot, E. Normandeau, Y. Dorant, O. K. Tørresen, S. N. K. Hoff, S. Jentoft, P. Sirois, et al. 2020. Shared ancestral polymorphisms and chromosomal rearrangements as potential drivers of local adaptation in a marine fish. *Mol. Ecol.* 29:2379–98. doi:10.1111/mec.15499.
- Davenport, J., and A. Stene. 1986. Freezing resistance, temperature and salinity tolerance in eggs, larvae and adults of capelin, *Mallotus villosus*, from Balsfjord. *J. Mar. Biol* 66:145–57. doi:10.1017/s0025315400039710.
- Davenport, J., O. Vahl, and S. Lønning. 1979. Cold resistance in the eggs of the capelin *Mallotus villosus*. *J. Mar. Biol* 59:443–53. doi:10.1017/s0025315400042764.
- Eguíluz, V. M., J. Fernández-Gracia, X. Irigoien, and C. M. Duarte. 2016. A quantitative assessment of Arctic shipping in 2010–2014. *Sci. Rep* 6:30682. doi:10.1038/srep30682.
- Eide, M., X. Zhang, O. A. Karlsen, J. V. Goldstone, J. Stegeman, I. Jonassen, and A. Goksøyr. 2021. The chemical defensome of five model teleost fish. *Sci. Rep* 11:10546. doi:10.1038/s41598-021-89948-0.
- Eliasson, K., G. F. Ulfarsson, T. Valsson, and S. M. Gardarsson. 2017. Identification of development areas in a warming Arctic with respect to natural resources, transportation, protected areas, and geography. *Futures* 85:14–29. doi:10.1016/j.futures.2016.11.005.
- Esbaugh, A. J., E. M. Mager, J. D. Stieglitz, R. Hoenig, T. L. Brown, B. L. French, T. L. Linbo, C. Lay, H. Forth, N. L. Scholz, et al. 2016. The effects of weathering and chemical dispersion on deepwater Horizon crude oil toxicity to mahi-mahi (*Coryphaena hippurus*) early life stages. *Sci. Tot. Environ* 543:644–51. doi:10.1016/j.scitotenv.2015.11.068.
- Frantzen, M., I. -B. Falk-Petersen, J. Nahrgang, T. J. Smith, G. H. Olsen, T. A. Hangstad, and L. Camus. 2012. Toxicity of crude oil and pyrene to the embryos of beach spawning capelin (*Mallotus villosus*). *Aquat. Toxicol.* 108:42–52. doi:10.1016/j.aquatox.2011.09.022.

- Goldstone, J. V., A. Hamdoun, B. J. Cole, M. Howard-Ashby, D. W. Nebert, M. Scally, M. Dean, D. Epel, M. E. Hahn, and J. J. Stegeman. 2006. The chemical defensome: Environmental sensing and response genes in the *Strongylocentrotus purpuratus* genome. *Develop. Biol* 300:366–84. doi:10.1016/j.ydbio.2006.08.066.
- González-Penagos, C. E., J. A. Zamora-Briseño, M. Améndola-Pimenta, J. M. Elizalde-Contreras, F. Árcaga-Cabrera, Y. Cruz-Quintana, A. M. Santana-Piñeros, M. A. Cañizález-Martínez, J. A. Pérez-Vega, E. Ruiz-May, et al. 2022. Integrative description of changes occurring on zebrafish embryos exposed to water-soluble crude oil components and its mixture with a chemical surfactant. *Toxicol. Appl. Pharm* 445:116033. doi:10.1016/j.taap.2022.116033.
- Greenacre, M. 2016. Data reporting and visualization in ecology. *Polar Biol.* 39:2189–205. doi:10.1007/s00300-016-2047-2.
- Greer, J. B., C. Pasparakis, J. D. Stieglitz, D. Benetti, M. Grosell, and D. Schlenk. 2019. Effects of corexit 9500A and Corexit-crude oil mixtures on transcriptomic pathways and developmental toxicity in early life stage mahi-mahi (*Coryphaena hippurus*). *Aquat. Toxicol.* 212:233–40. doi:10.1016/j.aquatox.2019.05.014.
- Hansen, B. H., T. Nordtug, J. Farkas, E. A. Khan, E. Oteri, B. Kvæstad, L. -G. Faksness, P. S. Daling, and A. Arukwe. 2021. Toxicity and developmental effects of Arctic fuel oil types on early life stages of Atlantic cod (*Gadus morhua*). *Aquat. Toxicol.* 237:105881. doi:10.1016/j.aquatox.2021.105881.
- Hansen, B. H., T. Parkerton, T. Nordtug, T. R. Størseth, and A. Redman. 2019. Modeling the toxicity of dissolved crude oil exposures to characterize the sensitivity of cod (*Gadus morhua*) larvae and role of individual and unresolved hydrocarbons. *Mar. Pollut. Bull.* 138:286–94. doi:10.1016/j.marpolbul.2018.10.065.
- Hicken, C. E., T. L. Linbo, D. H. Baldwin, M. L. Willis, M. S. Myers, L. Holland, M. Larsen, M. S. Stekoll, S. D. Rice, T. K. Collier, et al. 2011. Sublethal exposure to crude oil during embryonic development alters cardiac morphology and reduces aerobic capacity in adult fish. *PNAS* 108:7086–90. doi:10.1073/pnas.1019031108.
- Hop, H., and H. Gjøsæter. 2013. Polar cod (*Boreogadus saida*) and capelin (*Mallotus villosus*) as key species in marine food webs of the Arctic and the Barents Sea. *Mar. Biol. Res* 9:878–94. doi:10.1080/17451000.2013.775458.
- Hreinsson, H., 2020. The increase in arctic shipping 2013-2019 - arctic shipping status report (ASSR) #1, Arctic Council. <https://policycommons.net/artifacts/2233164/the-increase-in-arctic-shipping-2013-2019/2991094/on13Dec2022.CID:20.500.12592/j1qtwk>
- Incardona, J. P., M. G. Carls, H. L. Day, C. A. Sloan, J. L. Bolton, T. K. Collier, and N. L. Scholz. 2009. Cardiac arrhythmia is the primary response of embryonic pacific herring (*Clupea pallasii*) exposed to crude oil during weathering. *Environ. Sci. Technol* 43:201–07. doi:10.1021/es802270t.
- Incardona, J. P., M. G. Carls, L. Holland, T. L. Linbo, D. H. Baldwin, M. S. Myers, K. A. Peck, M. Tagal, S. D. Rice, and N. L. Scholz. 2015. Very low embryonic crude oil exposures cause lasting cardiac defects in salmon and herring. *Sci. Rep* 5:13499. doi:10.1038/srep13499.
- Incardona, J. P., L. D. Gardner, T. L. Linbo, T. L. Brown, A. J. Esbaugh, E. M. Mager, J. D. Stieglitz, B. L. French, J. S. Labenia, C. A. Laetz, et al. 2014. Deepwater Horizon crude oil impacts the developing hearts of large predatory pelagic fish. *PNAS* 111:E1510–8. doi:10.1073/pnas.1320950111.
- Incardona, J. P., T. L. Linbo, B. L. French, J. Cameron, K. A. Peck, C. A. Laetz, M. B. Hicks, G. Hutchinson, S. E. Allan, D. T. Boyd, et al. 2021. Low-level embryonic crude oil exposure disrupts ventricular ballooning and subsequent trabeculation in Pacific herring. *Aquat. Toxicol.* 235:105810. doi:10.1016/j.aquatox.2021.105810.
- Incardona, J. P., and N. L. Scholz. 2016. The influence of heart developmental anatomy on cardiotoxicity-based adverse outcome pathways in fish. *Aquat. Toxicol.* 177:515–25. doi:10.1016/j.aquatox.2016.06.016.
- Lie, K. K., S. Meier, E. Sørhus, R. B. Edvardsen, Ø. Karlsen, and P. A. Olsvik. 2019. Offshore crude oil disrupts retinoid signaling and eye development in larval Atlantic Haddock. *Frontiers. Mar. Sci* 6:368. doi:10.3389/fmars.2019.00368.
- Lønning, S. 1981. Comparative electron microscope studies of the chorion of the fish egg. *Rapp. P.-V. Cons. Int. Explor. Mer* 178:560–64.
- Lønning, S., E. Kjørsvik, and I. B. Falk-Petersen. 1988. A comparative study of pelagic and demersal eggs from common marine fishes in Northern Norway. *Sarsia* 73:49–60. doi:10.1080/00364827.1988.10420671.
- Mager, E. M., A. J. Esbaugh, J. D. Stieglitz, R. Hoenig, C. Bodinier, J. P. Incardona, N. L. Scholz, D. D. Benetti, and M. Grosell. 2014. Acute embryonic or juvenile exposure to deepwater horizon crude oil impairs the swimming performance of mahi-mahi (*Coryphaena hippurus*). *Environ. Sci. Technol* 48:7053–61. doi:10.1021/es501628k.
- McIntosh, S., T. King, D. Wu, and P. V. Hodson. 2010. Toxicity of dispersed weathered crude oil to early life stages of Atlantic herring (*Clupea harengus*). *Environ. Toxicol. Chem.* 29:1160–67. doi:10.1002/etc.134.
- Meador, J. P., and J. Nahrgang. 2019. Characterizing crude oil toxicity to early-life stage fish based on a complex mixture: Are we making unsupported assumptions? *Environ. Sci. Technol* 53:11080–92. doi:10.1021/acs.est.9b02889.
- Melbye, A. G., O. G. Brakstad, J. N. Hokstad, I. K. Gregersen, B. H. Hansen, A. M. Booth, S. J. Rowland, and K. E. Tollefsen. 2009. Chemical and toxicological characterization of an unresolved complex mixture-rich biodegraded crude oil. *Environ. Toxicol. Chem.* 28:1815–24. doi:10.1897/08-545.1.
- Nahrgang, J., P. Dubourg, M. Frantzen, D. Storch, F. Dahlke, and J. P. Meador. 2016. Early life stages of an arctic keystone species (*Boreogadus saida*) show high sensitivity to a water-soluble fraction of crude oil. *Environ. Pollut.* 218:605–14. doi:10.1016/j.envpol.2016.07.044.

- Paine, M. D., W. C. Leggett, J. K. McRuer, and K. T. Frank. 1992. Effects of Hibernia crude oil on Capelin (*Mallotus villosus*) embryos and larvae. *Mar. Environ. Res.* 33:159–87. doi:10.1016/0141-1136(92)90147-e.
- Pasparakis, C., A. J. Esbaugh, W. Burggren, and M. Grosell. 2019. Physiological impacts of Deepwater Horizon oil on fish. *Comp. Biochem. Physiol. C, Comp. Pharmacol.* 224:108558. doi:10.1016/j.cbpc.2019.06.002.
- Perrichon, P., C. E. Donald, E. Sørhus, T. Harboe, and S. Meier. 2021. Differential developmental toxicity of crude oil in early life stages of Atlantic halibut (*Hippoglossus hippoglossus*). *Sci. Total Environ.* 770:145349. doi:10.1016/j.scitotenv.2021.145349.
- Petersen, K., M. T. Hultman, S. J. Rowland, and K. E. Tollefsen. 2017. Toxicity of organic compounds from unresolved complex mixtures (UCMs) to primary fish hepatocytes. *Aquat. Toxicol.* 190:150–61. doi:10.1016/j.aquatox.2017.06.007.
- Pinheiro, J., D. Bates, and R Core Team (2023). Nlme: Linear and Nonlinear Mixed Effects Models. *R package version 3.1-162*. <https://CRAN.R-project.org/package=nlme>
- Præbel, K., J. S. Christiansen, and S. E. Fevolden. 2009. Temperature and salinity conditions in a sub-Arctic intertidal spawning habitat for capelin. *Mar. Biol. Res* 5:511–14. doi:10.1080/17451000902729670.
- Præbel, K., J. S. Christiansen, A. Kettunen-Præbel, and S. E. Fevolden. 2013. Thermohaline tolerance and embryonic development in capelin eggs (*Mallotus villosus*) from the Northeast Atlantic Ocean. *Environ. Biol. Fish* 96:753–61. doi:10.1007/s10641-012-0069-3.
- R Core Team. 2022. *R: A language and environment for statistical computing*. Vienna, Austria: R Foundation for Statistical Computing. <https://www.R-project.org/>.
- Sammarco, P. W., S. R. Kolian, R. A. F. Warby, J. L. Bouldin, W. A. Subra, and S. A. Porter. 2013. Distribution and concentrations of petroleum hydrocarbons associated with the BP/Deepwater Horizon Oil Spill, Gulf of Mexico. *Mar. Pollut. Bull.* 73:129–43. doi:10.1016/j.marpolbul.2013.05.029.
- Shadrin, A. M., V. V. Makhotin, and E. Eriksen. 2020. Incubation Temperature effect on qualitative and quantitative composition of abnormalities and mortality rate in embryogenesis of the barents sea capelin *Mallotus villosus* (Osmeridae). *J. Ichthyol* 60:79–89. doi:10.1134/s0032945220010142.
- Smith, L. C., and S. R. Stephenson. 2013. New trans-Arctic shipping routes navigable by midcentury. *PNAS* 110: E1191–95. doi:10.1073/pnas.1214212110.
- Sørensen, L., B. H. Hansen, J. Farkas, C. E. Donald, W. J. Robson, A. Tonkin, S. Meier, and S. J. Rowland. 2019. Accumulation and toxicity of monoaromatic petroleum hydrocarbons in early life stages of cod and haddock. *Environ. Pollut.* 251:212–20. doi:10.1016/j.envpol.2019.04.126.
- Sørensen, L., S. Meier, and S. A. Mjøs. 2016. Application of gas chromatography/tandem mass spectrometry to determine a wide range of petrogenic alkylated polycyclic aromatic hydrocarbons in biotic samples. *Rapid Commun. Mass Spectrom.* 30:2052–58. doi:10.1002/rcm.7688.
- Sørensen, L., M. S. Silva, A. M. Booth, and S. Meier. 2016. Optimization and comparison of miniaturized extraction techniques for PAHs from crude oil exposed Atlantic cod and haddock eggs. *Anal. Bioanal. Chem* 408:1023–32. doi:10.1007/s00216-015-9225-x.
- Sørensen, L., E. Sørhus, T. Nordtug, J. P. Incardona, T. L. Linbo, L. Giovanetti, Ø. Karlsen, S. Meier, and I. Corsi. 2017. Oil droplet fouling and differential toxicokinetics of polycyclic aromatic hydrocarbons in embryos of Atlantic haddock and cod. *PLoS One* 12:e0180048. doi:10.1371/journal.pone.0180048.
- Sørhus, E., C. E. Donald, D. Silva da, A. Thorsen, Ø. Karlsen, and S. Meier. 2021. Untangling mechanisms of crude oil toxicity: Linking gene expression, morphology and PAHs at two developmental stages in a cold-water fish. *Sci. Total Environ.* 757:143896. doi:10.1016/j.scitotenv.2020.143896.
- Sørhus, E., R. B. Edvardsen, Ø. Karlsen, T. Nordtug, T. van der Meeren, A. Thorsen, C. Harman, S. Jentoft, S. Meier, and I. Corsi. 2015. Unexpected interaction with dispersed crude oil droplets drives severe toxicity in Atlantic haddock embryos. *PLoS One* 10:e0124376. doi:10.1371/journal.pone.0124376.
- Sørhus, E., S. Meier, C. E. Donald, T. Furmanek, R. B. Edvardsen, and K. K. Lie. 2021. Cardiac dysfunction affects eye development and vision by reducing supply of lipids in fish. *Sci. Total Environ.* 800:149460. doi:10.1016/j.scitotenv.2021.149460.
- Spurgeon, D., E. Lahive, A. Robinson, S. Short, and P. Kille. 2020. Species sensitivity to toxic substances: Evolution, ecology and applications. *Frontiers. Environ. Sci* 8:588380. doi:10.3389/fenvs.2020.588380.
- Stuart, K. R., and M. Drawbridge. 2011. The effect of light intensity and green water on survival and growth of cultured larval California yellowtail (*Seriola lalandi*). *Aquaculture* 321:152–56. doi:10.1016/j.aquaculture.2011.08.023.
- Tairova, Z., M. Frantzen, A. Mosbech, A. Arukwe, and K. Gustavson. 2019. Effects of water accommodated fraction of physically and chemically dispersed heavy fuel oil on beach spawning capelin (*Mallotus villosus*). *Mar. Environ. Res.* 147:62–71. doi:10.1016/j.marenvres.2019.03.010.